6-2013

Maximum Power Point Tracking Device for a Photovoltaic Panel

Betsy Schwartz
Union College - Schenectady, NY

Maximum Power Point Tracking Device for a Photovoltaic Panel

By

Betsy Schwartz

* * * * * * * * * * * * * * * * *

Submitted in partial fulfillment
of the requirements for
Honors in the Department of Electrical and Computer Engineering

Union College
June, 2013

Abstract

SCHWARTZ, BETSY Maximum Power Point Tracking Device for a Photovoltaic Panel. Department of Electrical and Computer Engineering, June 2013.

ADVISOR: Professor Robert Smith

The operating characteristics of a photovoltaic (PV) solar panel are dependent upon the lighting and temperature conditions, as well as the characteristics of the energy storage device and/or loads that it feeds. PV panels normally operate at a fixed voltage and current for a given load and sunlight condition. The operating conditions will not necessarily produce the maximum possible power output of a solar panel for the set conditions. The efficiency of power delivery from a PV panel can be greatly increased by a Maximum Power Point Tracker (MPPT). An algorithm can be designed to shift the operating value to the maximum power point (MPP). A DC-to-DC converter can then be built to provide a battery with the highest possible power from the PV panel.

In this project, the current and voltage output of a PV panel are measured and provided to a controller that continuously adjusts the PV operating point to produce the greatest average power output. The controller controls the duty cycle of a switch-mode DC-to-DC converter, which in turn provides a pulse-width-modulated (PWM) output to a battery bank. The converter will thus more closely match the battery's storage impedance and provide a voltage that is proper to charge the battery. After testing, the system was able to operate at times near its maximum power but due to sampling issues this was not always the case.

Table of Contents

1. List of Figures

2. List of Tables

3. Introduction

Solar cells have become increasingly popular as a source of renewable energy. To work most efficiently, a PV panel should operate at the point which produces the greatest output power, referred to as the maximum power point (MPP). The MPP is found by obtaining a characteristic IV curve for the device, which is a plot of current versus voltage, as shown in Figure 1. The maximum possible voltage on the curve corresponds to the open circuit voltage and the maximum current corresponds to the short circuit current of the panel. The IV curve is plotted by applying varying loads to the PV cell and measuring its current and voltage output. This curve will be different for each PV cell and will also depend on the outdoor conditions of sun intensity, known as irradiance (measured in watts per square meter), and temperature. For any given intensity and temperature curve, the operating point will be a function of the impedance seen by the cell's output. Therefore, it is not as simple as finding the MPP for the cell and always operating at this point to get the highest power. Instead a Maximum Power Point Tracking device must be used that will continuously examine the conditions and find the changing MPP. For the system to operate at many points along an IV curve the switching of the circuit must be able to operate in many different states rather than just on and off. Having the ability to operate the switch as a varying resistor allows for changing impedance values of the circuit, resulting in the ability to perturb along the IV curve.

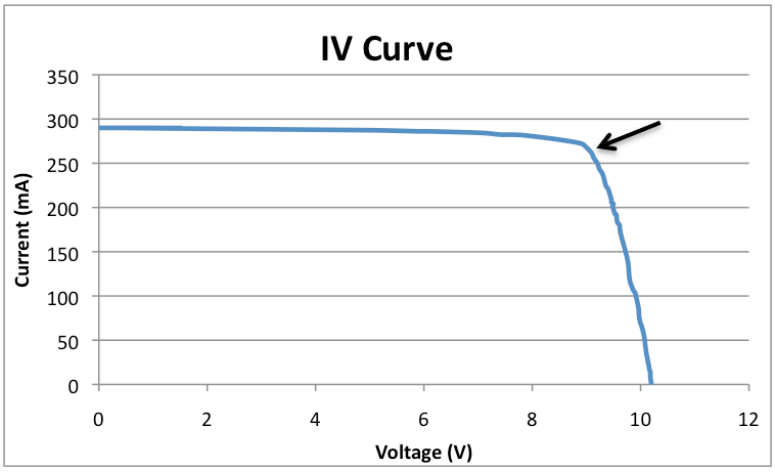

Figure 1: IV curve showing the MPP

In a DC-to-DC converter, shown in Figure 2, in which the switch is always completely on or off, the operating conditions of the solar panel will be between two points on the IV curve; one point is at the open circuit condition when the switch is open and another when the switch is closed. The amount of time spent at each of these points can be averaged to find an average power value. In this case, the maximum power point will be on a straight line that can be drawn connecting the on and off operating points on the IV curve. Shown in Figure 3 is an IV curve and added line of time-averaged voltage and current depending on the duty cycle. The MPP of this straight line is obtained by finding the current and voltage pair whose product is the greatest. It should be noted that this is the maximum of the time-averaged power, which will not necessarily be at the PV panel's characteristic MPP.

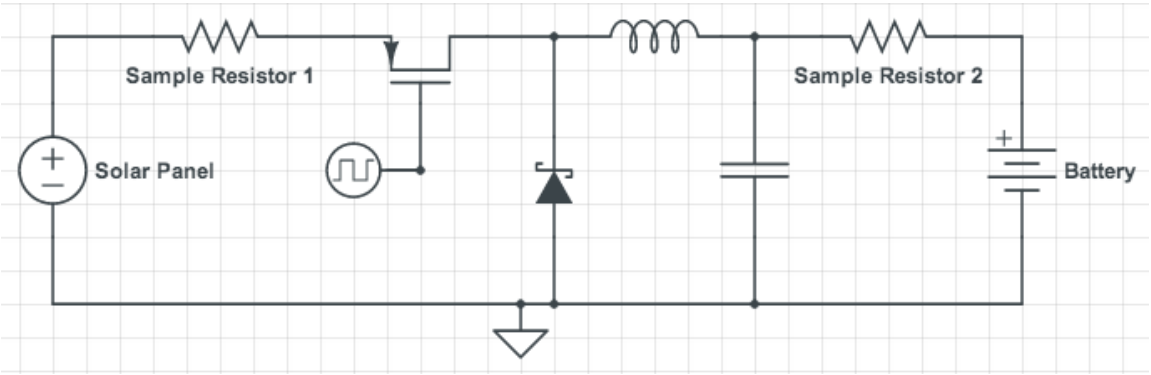

Figure 2: DC-DC Buck Converter

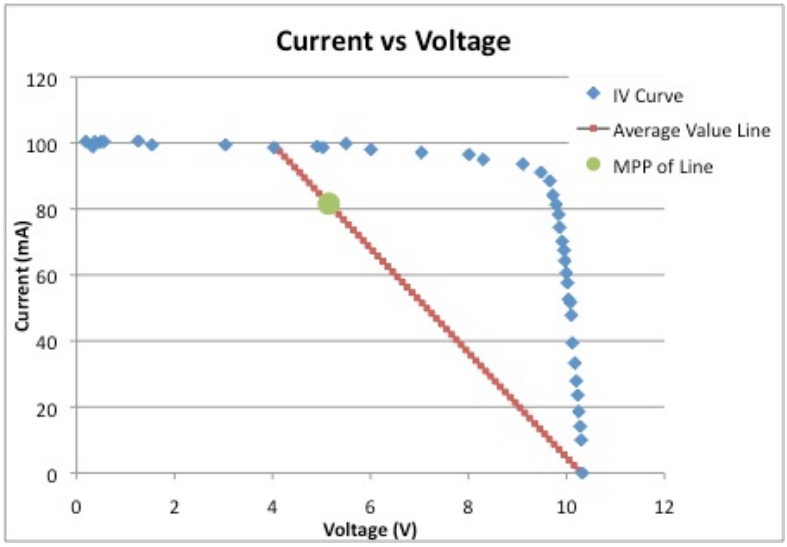

Figure 3: IV curve with time-averaged IV line

There are many different algorithms that can be used to find the MPP. Two of the most commonly used are Perturb & Observe (P&O) and Incremental Conductance (IC); these are both explained in the alternative design section. Depending on the voltage of the battery and the MPP voltage, a buck or boost DC-to-DC converter is needed to step the voltage up or down. Furthermore, if the PV cell's power is being fed into the grid a DC-to-AC inverter is needed. The rest of the paper will discuss background on the subject, specifications for the project, alternative designs, the final design and results.

4. Background

This section will first look at the history of MPPT devices and what has already been done in the field. Then, ideas are presented of how solar panels affect society in terms of the following issues: economic, environmental, sustainability, manufacturability, ethical and health and safety.

Maximum Power Point Tracking devices are continuously being developed and improved upon for photovoltaic systems. Papers began to be published on this topic in the late 1980's; since then many engineers have developed increasingly complex MPPT systems [1]. The goal of these devices is to optimize the power output of a solar cell by finding the value where the product of current and voltage is the greatest. For each cell this will be a slightly different value, due to the characteristics and placement of the solar cell. The temperature also plays a role in the optimal power point. MPPT systems are now built into some solar cells to operate at their most energy efficient point no matter the conditions; others are separate units that can be attached to a PV panel.

The United States has become more interested in developing its renewable energy resources, and solar energy is one of the main areas of discussion. The sun has the ability to produce steady power to the point where, if it could all be captured, it would be enough to be the world's single source of electricity [2]. Currently the price of solar panels is too high to be able to come close to this. If all solar panels were operating at their MPP the efficiency of the energy captured would increase electricity generation. Currently many newer solar panels have a built-in MPPT, but older types and small inexpensive panels are not likely to have them.

However, there are some negatives associated with PV panels. The placement of a solar panel can have an impact on society. With the current PV panel options, the physical size of the panel compared to the power out is very high. This is why it is especially important for the panel to operate efficiently. To generate a lot of power many of these large panels are needed, which can impact the area in which they are placed, not only in terms of what people might find aesthetically unappealing but also to wildlife. To generate large-scale power entire fields might be filled with freestanding PV panels. When this large area of land is cleared for the installation of the panels it could disrupt the ecosystem [2].

In the production of PV panels, hazardous materials may be created. For example, if a manufacturer is neglecting to take the proper steps with the byproducts of creating these panels, they could become harmful to society. PV panels may also be of harm if used incorrectly or disposed of improperly [3]. But if the manufacturer and user are handling the panel properly, there should only be minimal harmful effects to society.

Currently solar panels are one of the most expensive means of alternative energy. Many PV panels are being manufactured overseas, but advances in the technology and efficiency of the devices create more job opportunities within the US. With an increased use of solar panels, jobs will be created in many areas such as delivering the PV panels, installing them and making repairs. If care is put into the handling and planning of installation, the advantages of solar generation outnumber the negative effects. As the Unites States continues to invest more in renewable energy resources the sustainability of the country will be increased partly by the usage of solar panels.

There is current research to find a generic solution to reach the MPP as quickly and simply as possible. One innovative system uses a simple algorithm and switch that is able to find in one-step the approximate optimal point by locating the global maxima [5]. This technique has effectively reduced the complexity and cost of accurate MPPT methods. Research in this field will continue to find the best way to maximize the power output in solar cell applications.

5. Design Requirements

In this section, methods of measuring the project's effectiveness will be presented, along with other aspects such as users and cost. The major requirement of the system is that the final MPPT should be able to extract higher power output from a PV panel than is possible without a MPPT. Waveforms from the DC-to-DC converter alone will be captured to show that this component of the system is working as expected for known duty cycles. Likewise the control system can be tested with constant valued inputs to make sure it operates as expected. Overall success can be measured based on calculated MPP values from approximations made from data gathered for different lighting conditions, shown in appendix 16.1. Ideally the system will operate as closely as possible to the maximum power point the majority of the time, meaning it will not take long to find this point as the light changes.

The I/O card being used can only read in voltages between -10V and 10V, and since the solar panel has an open circuit voltage slightly larger than 10V (around 10.3V), these higher values will be read in as 10V. This is not a large constraint since this value only occurs right before the open circuit voltage is reached and will be far from the MPP. The computer's sampling capability plays a role in the ability of the control algorithm to properly sample the PV panel's input, when deciding whether to increase or decrease the duty cycle. To find the average voltage and current at the input of the PV panel, the sampling rate must be fast enough to gain an adequate representation of the sampled voltages.

The algorithm in Simulink can easily be used to program a microcontroller in another language. This will allow for a variety of packaging possibilities so the user will

not need to be particularly technically versed in MPPT technology. Anyone who wants to make a PV panel more efficient in power generation to charge a small battery can use the device. The algorithm will take care of charging and protecting the battery so the user does not have to worry about damaging the battery. The cost of the device will be relatively low for a user who already has a computer with MathWorks' Simulink software; if the program is put onto a microcontroller this will then be the main cost. The user's cost will be for an analog to digital I/O card and a small amount for the components in the circuitry.

6. Design Alternatives

This section concentrates on other ways of completing the project to reach the MPP of the IV curve. Different algorithms and DC-to-DC converter options will be explained. Each algorithm has its advantages and disadvantages, with tradeoffs between efficiency and ease of implementation.

6.1 Algorithm Alternatives

There are many different algorithms that have been used to find the MPP. One common method is Perturb & Observe (P&O). This method works by varying the output voltage of the solar cell by changing the PWM duty cycle of the converter and measuring the average PV output power at that voltage. This algorithm is used with a circuit having the ability to match the impedance of the solar panel for maximum power transfer. If the power is greater than that of the previous point it continues perturbing in that direction; if the power has decreased it then varies the voltage in the opposite direction. Since the sunlight can change at any moment it is also necessary to check whether or not the voltage has increased or decreased. To arrive at the MPP the duty cycle is decreased if the product of power and voltage changes is positive and increased otherwise. Then the device will switch back and forth between one step above and one below the desired point [6]. One of the downfalls with this method is that when the sunlight conditions are quickly changing the device might have difficulty finding the MPP as it is searching for the point [7]. This technique is relatively easy to implement but is not able to track the MPP as quickly as others and will oscillate slightly around the MPP.

Another method is Incremental Conductance (IC), which examines the slope of the power curve. On the power curve the MPP is going to be at its maximum when the

slope is zero, corresponding to Eq. (1). When the change in power is positive this is a point on the curve which is to the left of the MPP, when the slope of the power curve is negative the point has been passed. From this an algorithm can be formed comparing the incremental conductance to the instantaneous conductance. At MPP the incremental conductance is given by Eq. (2). Equation's (3) and (4) give the incremental conductance to the right and left of the MPP, respectively [6].

$$\frac{dP}{dV} = \frac{d(VI)}{dV} = I\frac{dV}{dV} + V\frac{dI}{dV} = 0 \qquad (1)$$

$$\frac{dI}{dV} = -\frac{I}{V} \qquad (2)$$

$$\frac{dI}{dV} < -\frac{I}{V} \qquad (3)$$

$$\frac{dI}{dV} > -\frac{I}{V} \qquad (4)$$

Once the MPP is located it is held at this point until the sun's intensity changes. Similar to the P&O method the IC method needs both current and voltage values, but IC has a more complex implementation. This method is effective for rapidly changing lighting conditions [7]. A PI controller can be used to decrease this method's response time by using large steps when far from the MPP, and smaller steps around the desired point [6].

The Short-Current Pulse (SC) method uses the short circuit current and the sunlight conditions to estimate the optimal current for MPP. To find the short circuit current a switch is used in parallel to briefly short circuit the solar array. Some energy is lost as the power of the PV panel is at zero while the voltage is set to zero to find the short circuit current. The proportionality factor for the short circuit to optimal current varies based on the temperature; it is around 0.92. This method allows for calculation of

the optimal current by finding the short circuit current in a specific lighting condition and multiplying it by the proportionality factor [7].

Similarly, the Open Voltage (OV) method uses the same concept as SC but using the PV open-circuit voltage. It is assumed that the open circuit voltage is always roughly proportional to the MPP voltage by a factor of about 0.76. To find the open voltage a switch is used in series with the solar array. In this case, some energy is lost as the power of the PV is at zero, while the current is set to zero to find the open circuit voltage. When the open circuit voltage at a certain lighting condition is multiplied by the proportionality factor, the voltage for the MPP is calculated [7].

Tradeoffs between the methods come from cost, ease of implementation and execution speed. P&O is very simple and easy to use but its speed is an issue for quickly changing environments. IC is often used for its speed, tracking rapidly changing conditions, although it is more expensive and slightly more complicated [6]. SC and OV methods rely on proportionality factors that vary with each specific solar cell and can therefore produce unreliable results. The IC method has even better results when the step size of measurements is variable; it is able to rapidly find changing MPP's [8].

6.2 Circuitry Alternatives

After the MPP is located by one of the previous methods, the power from the solar panel needs to be adjusted based on what battery and/or load it is connected to. For a system connected to the grid the voltage will have to be converted to an AC signal. If the output energy is being stored in a battery it will need to go through a converter to match the fixed DC voltage of the battery. Depending on the voltage at the MPP it will either need to pass through a buck or boost converter. If the MPP voltage is larger than

the battery's voltage, in order to store the energy the voltage must be reduced with a buck converter; if the opposite is the case a boost converter is used to bring up the MPP voltage to the battery's voltage. Some MPPT systems that charge DC devices use a combination buck-boost system which can act as a buck or boost converter depending on the situation [4]. If the DC-to-DC converter used were a buck-boost, by adjusting the values of the components the same configuration could be used to charge different batteries with other types of solar panels. The converters are implemented with a switch that works via a varying duty cycle, diode, inductor and capacitor across the load [4].

7. Final Design and Implementation

This section will provide detail on how the project was constructed and how the component values were determined. The implemented circuit does not exactly match the impedance of the solar panel to the battery circuit, but instead finds the MPP along a line that connects the two PV operating points, on the IV curve, when the switch is open and closed. Originally the plan was to create an impedance matching device which could locate the MPP along the systems IV curve in an analog fashion. After a last minute realization, it was made clear that this system is not able to do this as designed so the project instead aims to maximize the power along a straight line with end points on the IV curve when the switch is open and when closed. For any particular lighting and temperature condition, these are the only two impedances which the circuit can operate at, rather than at many different impedances along the IV curve.

The solar panel to be used in the project was provided without any specification sheets. Thus, the open circuit voltage and short circuit current for various lighting conditions and loads needed to be measured to characterize the panel's capabilities. Originally the work was performed outside, at which point it was realized that the sunlight intensity varied too greatly to plot an accurate IV curve. Instead, a halogen light was set up to take the measurements in a controlled lab environment; see appendix section 16.1 for the plotted IV curves. With measured voltages and currents out of the solar panel for the each lighting condition when the switch is both open and closed, the straight line can be plotted and the MPP along this line located. This is the value which the system will aim to operate at. With the MPP of the average IV line known for a few different levels of lighting a battery and DC-to-DC converter topology could be selected

for this particular panel. The battery was chosen to be a 3.7V, 950mAh Lithium-Ion Polymer cell phone battery. Since the battery's voltage is lower than the voltage of the MPP, a buck converter was used to step down the panel's voltage to safely charge it.

For a specific load and light condition the panel will operate at a certain point on its IV curve; in order to change that operating point the average voltage is perturbed by an algorithm. Adjusting the duty cycle of the switching transistor in the DC-to-DC converter causes a change in the impedance of the circuit between two states. The pulse width modulated signal is generated in Simulink with a triangle wave at the desired PWM frequency, chosen to be 2 kHz, and a DC reference voltage. By changing the reference voltage the duty cycle can be varied. This is how the algorithm moves the average operating conditions of the panel. The voltage across the PV panel and its output current are read into Simulink through an input/output (I/O) card in the host computer. The power is calculated from the current and voltage inputs and then compared to the previous power [6]. The full block diagram with control system and circuitry is seen in Figure 4. Once the PWM signal is generated in the computer it is transmitted to the I/O card, from which it serves as the input to the switching MOSFET of the DC-to-DC converter.

7.1 Algorithm

Figure 5 shows the flowchart of the algorithm as constructed in Simulink. Initially the voltage at the PV panel is measured and the current through a test resistor is calculated, giving a value for the power from the solar panel. Then the initial duty cycle of the PWM signal is arbitrarily set to 50%. The voltage and current are again measured

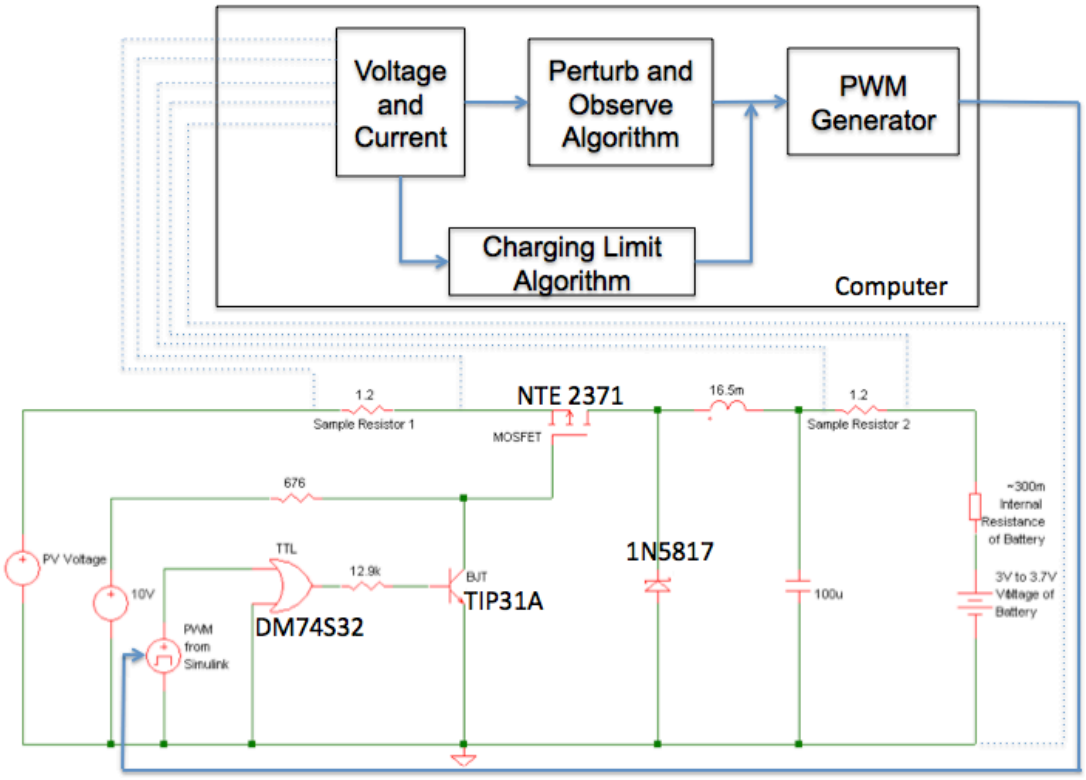

Figure 4: MPPT block diagram

to obtain the PV output power. Now the power and voltages are compared to the previous step to see if they have increased or decreased. By examining the signs of these increments, the algorithm determines whether the perturbation of the duty cycle caused a move toward, or away from, the maximum power point. Between the four different combinations of increasing or decreasing voltage and power, the control system will either call for an increase or decrease in the duty cycle of the PWM signal. The duty cycle is adjusted by generating a DC reference between 0 and 1 to be compared to a triangle wave. Once the initial value is set the constant adjusts in steps of +/-0.05 per perturbation.

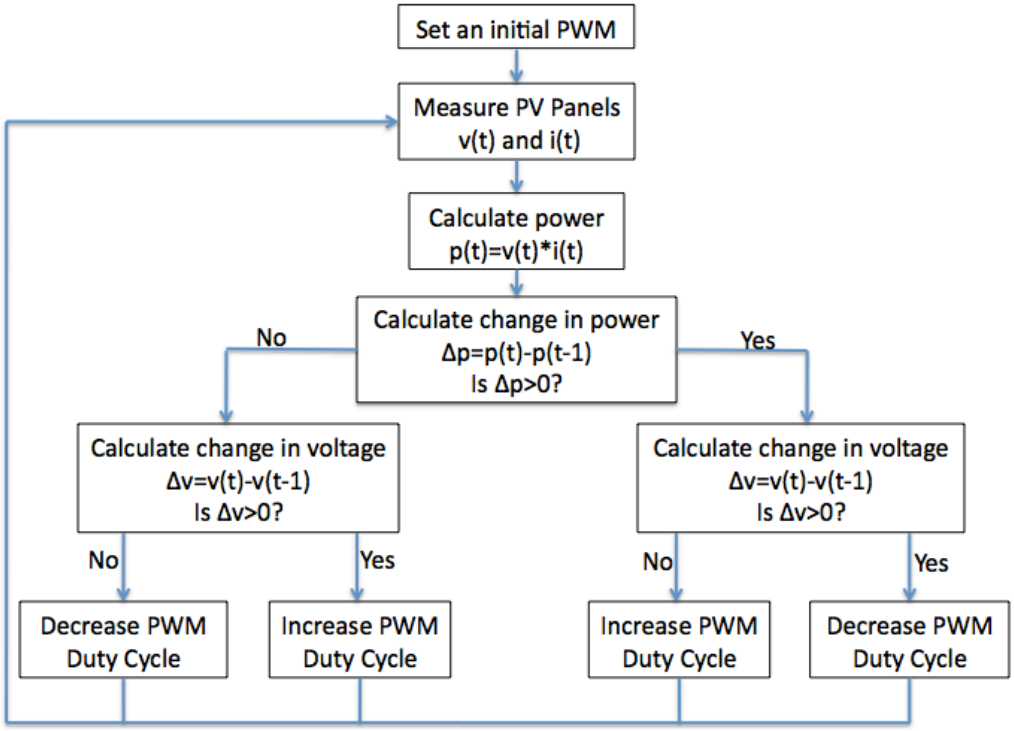

Figure 5: Logic flowchart

Above all else there is a battery limit algorithm to make sure the battery is being safely charged. If the current gets as high as 500mA or the battery's voltage is above 3.7V, the MPP will no longer govern the algorithm's behavior, but instead the current to the battery will be decreased by reducing the PWM duty cycle so the battery is not damaged. The charging current limit was taken from battery literature [9]. In this way once the battery is fully charged, the algorithm will adjust to a 0% duty cycle at which point no current is getting to the battery.

To generate a fast switching rate, which reduces the physical size of the circuit components that are needed, the triangle wave and subsequently the PWM signal are generated at 2 kHz. It is not necessary for the PV panel's voltage and current outputs to be measured at this rate since the sunlight does not change this quickly and it was

discovered that the laboratory computer used could not read analog inputs at a rate near 2 kHz. The input voltage at the PV panel varies as the switch is opened and closed by the duty cycle. In order to decide whether the voltage has increased or decreased the average voltage over a period is needed. For this reason the placement of the sampling time must occur at a slightly different location during a cycling period with each sample. If the voltage of the solar panel were checked every 10 seconds exactly, the sampling would occur at the same location of a 2 kHz signal each time. That is why a sampling rate of (1/10.00005) Hz was chosen. This way after 10 samples there will be enough data to calculate the average voltage. After the first sample, 2000 cycles will have occurred and then the second sample will be one tenth of the way into the period, then another 2000 cycles will pass before the third sample is taken another tenth of the way into a period. After the 10^{th} sample there is enough knowledge to recreate a sample period of this waveform in order to calculate the average value, shown in Figure 6. After the 10 samples are read in and averaged, 100.0005 seconds will have passed. At this point the control algorithm chooses to increase or decrease the duty cycle and another set of 10 inputs are recorded and averaged. The full block diagram from Simulink can be seen in Appendix 16.2.

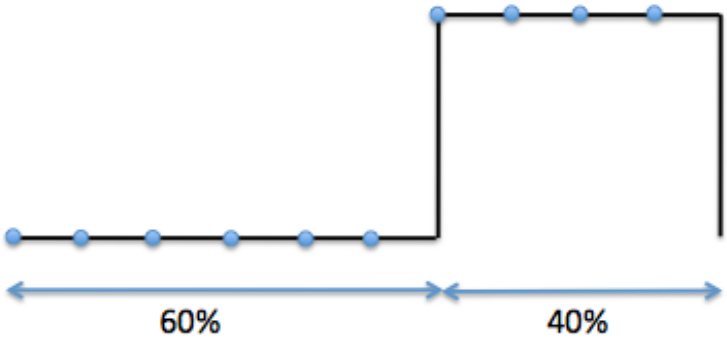

Figure 6: Sampling of PV panel input voltage

7.2 Circuitry

To initially calculate values for the capacitor and inductor shown in Figure 7, RLC circuit analysis was employed. When the switch is closed the voltage across the inductor is the difference between the input and output across the load (Eq. 5). When the switch is open the input is disconnected from the circuit and the voltage across the inductor is dependent on the voltage across the load and the diode's voltage drop (Eq. 6).

$$V_L = V_i - V_o \qquad (5)$$

$$V_L = -(V_o + V_d) \qquad (6)$$

In steady state the average voltage across the inductor during a switching period will be zero since an inductor cannot sustain a DC voltage. The integral of the voltage when the switch is opened added to the integral of the voltage when the switch is off must equal zero (Eq. 7). The switch is closed from time zero until time DT_s, which is the duty cycle multiplied by the switching period since the duty cycle is the fraction of time the switch is closed.

$$\int_0^{DT_s} (V_i - V_o)dt + \int_{DT_s}^{T_s} -(V_o + V_d)dt = 0 \qquad (7)$$

If the voltage across the load stays nearly constant, then Eq. 7 can be rewritten as Eq. 8. This is simplified to solve for the voltage across the load in Eq. 9 [10].

$$DT_s(V_i - V_o) - T_s(1 - D)(V_o + V_d) = 0 \qquad (8)$$

$$V_o = DV_i + (D - 1)V_d \qquad (9)$$

The inductor and capacitor are sized to limit ripple current. The current through the inductor will contain some amount of ripple at the switching frequency. The amount of ripple was chosen arbitrarily, to be limited to 10% - 15% of the nominal DC current which will be delivered to the load. For a fast switching transistor, the inductor is sized

with Eq. 10. The capacitor is there to limit even more of the current ripple from reaching the battery; the capacitance can be determined using Eq. 11. In solving for the capacitance the internal resistance of the battery, R_{INT}, must be known. From measurements in a fully charged battery (this is when the resistance is lowest), the battery's internal resistance was determined to be approximately 300mΩ.

$$L \geq \frac{(V_i - V_o)\left(\frac{V_0 - V_d}{V_i - V_d}\right)T_s}{10\% I_L} \qquad (10)$$

$$C \geq \frac{1}{2\pi f_s (10\%) R_{INT}} \qquad (11)$$

Calculating a value for the inductor and capacitor is a rough estimate because the input voltage, output voltage across the load, and current through the inductor will all vary as the system is perturbed. In the original calculations, the MPP along an IV curve would occur between 8.5 and 9.5V, so V_i was set to 9V for use in Eq. 10. The output voltage to charge the battery will need to be around 4V. Lastly, the DC current through the inductor (which is also the DC current to the battery) using the given solar panel should be about 250 mA when the battery is dead and less as it begins to charge. For the purpose of calculating inductor and capacitor values, a switching frequency fs of 2 kHz was used. Although a frequency this fast is not necessary for a DC voltage system, a faster switching frequency reduces the size of the inductor and capacitor, since the frequency is factored in to the denominator of both equations. Solving for an inductor and capacitor value in Eq.'s 10 and 11, a 33mH inductor and a 3000µF capacitor were initially chosen.

The chosen 33mH inductor was actually a transformer with two sets of 33mH inductors. After experimenting with the circuit it was found that the inductor was too large for the application, making the L/R time constant too large. The two sets of windings were put in parallel, resulting in a 16.5mH inductor. The capacitor was also significantly decreased in size, to 100μF. Although the ripple was not eliminated the capacitor was able to reach full charge without taking too much current from charging the battery. The original capacitor was eliminating significant ripple but never reaching full charge, continuously taking current that should have been charging the battery.

The fundamental DC-to-DC converter used a p-channel MOSFET as the switch. In order to completely turn off the MOSFET the voltage of the PWM signal to the transistor needed to reach 10V. The PWM signal is the output of the Simulink program which is fed out of the computer through a digital port on the I/O card to the circuit. To isolate and protect the expensive I/O card, the signal first goes through a TTL logic gate. The properties of this logic gate are such that the PWM will vary between on and off states of 0 and 5V. This signal is not large enough to fully turn off the switching MOSFET, so a transistor level shifter with a BJT transistor was placed between these stages to make sure the MOSFET gate voltage got to 10V in order to turn off the MOSFET.

The complete circuit diagram is seen in Figure 7. The circuit uses a flyback diode to ensure continuous inductor current. The diode needs to be able to quickly react to the switching speed of the MOSFET. A Schottky diode was used since it has a low forward voltage drop, allowing for more efficient switching between its conducting and non-conducting states. The diode is in reverse bias while the MOSFET is closed and forward

bias while the switch is open. The forward bias state allows for current to travel in a loop from the charged capacitor, through the diode and then the inductor.

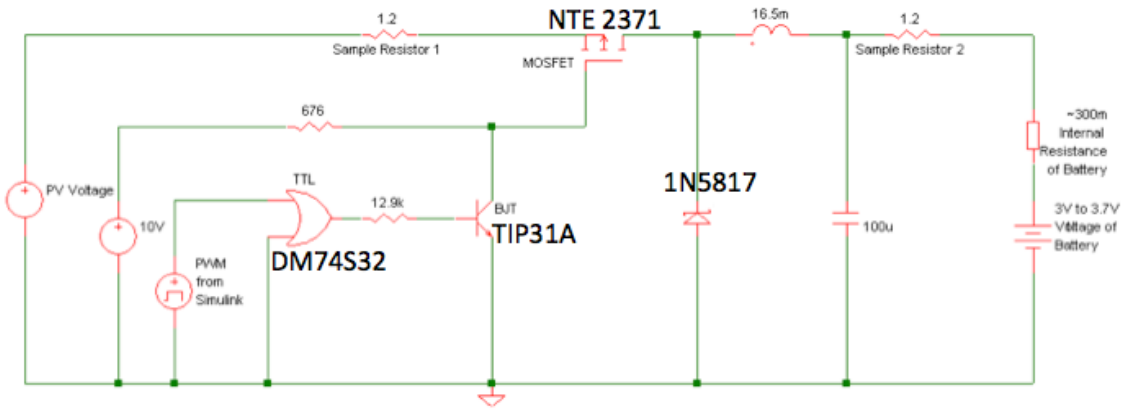

Figure 7: DC-to-DC circuit diagram

During the time which the MOSFET switch is opened, the PV panel's output is disconnected from the circuit and therefore operating at the open circuit voltage along the IV curve where no current is flowing. When the switch then closes, the current from the PV panel travels through the switch and inductor to the battery. Since there is now a large current the output of the PV panel is at a point on the IV curve with a voltage equal to the battery's plus any additional voltage drops due to resistors. Depending on the duty cycle of switching, the average power out of the PV panel will vary.

8. Performance Estimates and Results

The circuitry and control algorithm were initially each tested separately with a power supply as the input. As the power supply's voltage was changed, simulating the input voltage and current of the PV panel, the control system correctly adjusted the PWM duty cycle. This technique provided a limited look into the program since the voltage and current values were constantly being supplied to the algorithm and there was no need for sampling. When the full system was put together with the circuit, control system and solar panel, sampling issues did arise that made for difficulty reaching the MPP.

Waveforms from the working circuit can be seen in Figure 8. The pulse width modulated signal had a 40% duty cycle, meaning the MOSFET was closed for 40% of the time. This can be seen by looking at the PV input voltage, which is at a high level of about 10V for 60% of the time and just under 5V for the other 40% of the time. While the switch is open the PV input is disconnected from the charging battery, meaning the PV panel operates around the open circuit voltage. When the MOSFET then closes, the impedance that is seen by the PV panel decreases and it operates at a point where the voltage is equal to the battery's voltage plus any voltage drops across resistive devices. The diode is only needed while the MOSFET is open to allow current to travel from the capacitor through the diode and through the inductor. When the switch opens, the current through the inductor tries to quickly change which forward biases the diode as the inductor acts like a source. At the instant that the diode starts conducting there is a voltage of 0.4V across the diode and then after a brief oscillation period, the diode voltage stabilizes at the battery's voltage. When the switch then closes, the voltage across the diode shoots up to the voltage of the panel at 10V, and again oscillates before

leveling off at the battery's voltage until the switch reopens. These waveforms show that the circuit is working as expected.

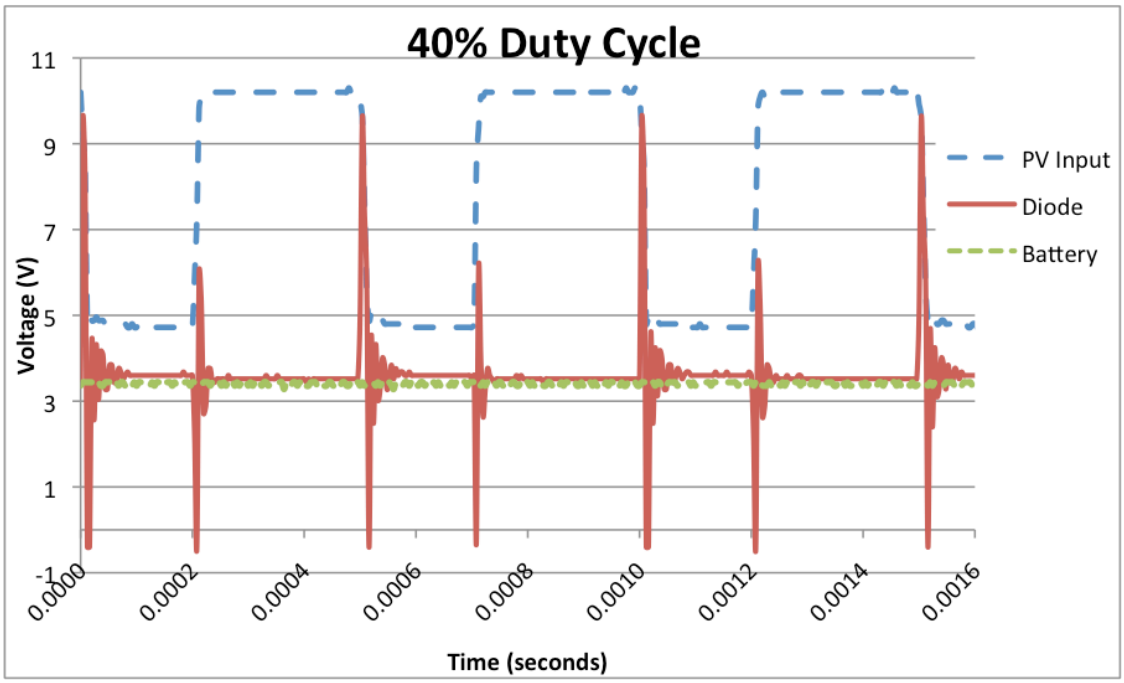

Figure 8: Waveforms with a 40% duty cycle PWM

When the battery is connected as the load to the DC-to-DC converter and the Simulink control algorithm is operational, the system often operates where expected but not always due to sampling problems. For lighting conditions with 200mA as a maximum the voltage should be between 5V and 6V. To more quickly see changes in the program, the sampling time was cut by a factor of 10 for testing purposes. The control system is successfully able to perturb the PV panel's average voltage, usually towards the time-averaged MPP. Figure 9 shows a snapshot over the course of 90 seconds of when the control panel has correctly located the time-averaged MPP and continues to operate at this value for the duration of the program, extending beyond the frame of this snapshot, until the battery is fully charged. The top waveform shows the average voltage at the solar panel between changes to the duty cycle. The middle plot is the voltage on the

other side of the test resistor, the MOSFET's source; here the voltage is slightly lower. Taking the difference in these voltages and dividing by the resistor's resistance of 1.2Ω, gives the current from the solar panel shown in the bottom plot. The last observed duty cycle in this snapshot was 95%.

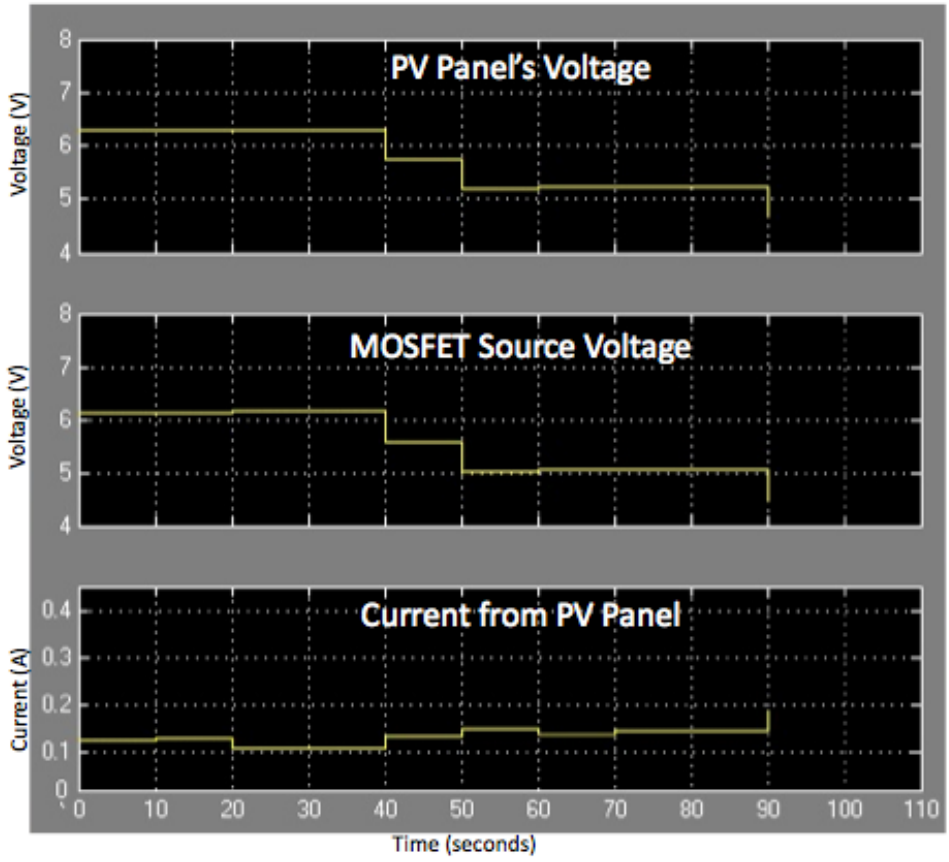

Figure 9: Simulink waveforms

At other times when the program is run, the current calculation coming from the PV panel is very high and not physically possible with the apparatus used. There is a problem with the sampling of the voltage at the test resistor on the MOSFET's source side. Although the PV Panel's voltage is being told to be read in at the same time and rate, the two waveforms appear different aside from the expected small voltage drop

when the switch is closed, shown in Figure 10. When these waveforms occur and then the average value is taken, the voltage at the source of the MOSFET is not a true representation and the average is therefore inaccurate. If this calculated average voltage is lower than what is expected, the current will subsequently appear much higher than it should. This throws off the algorithm from calculating an accurate power value and adjusting the duty cycle in the correct direction.

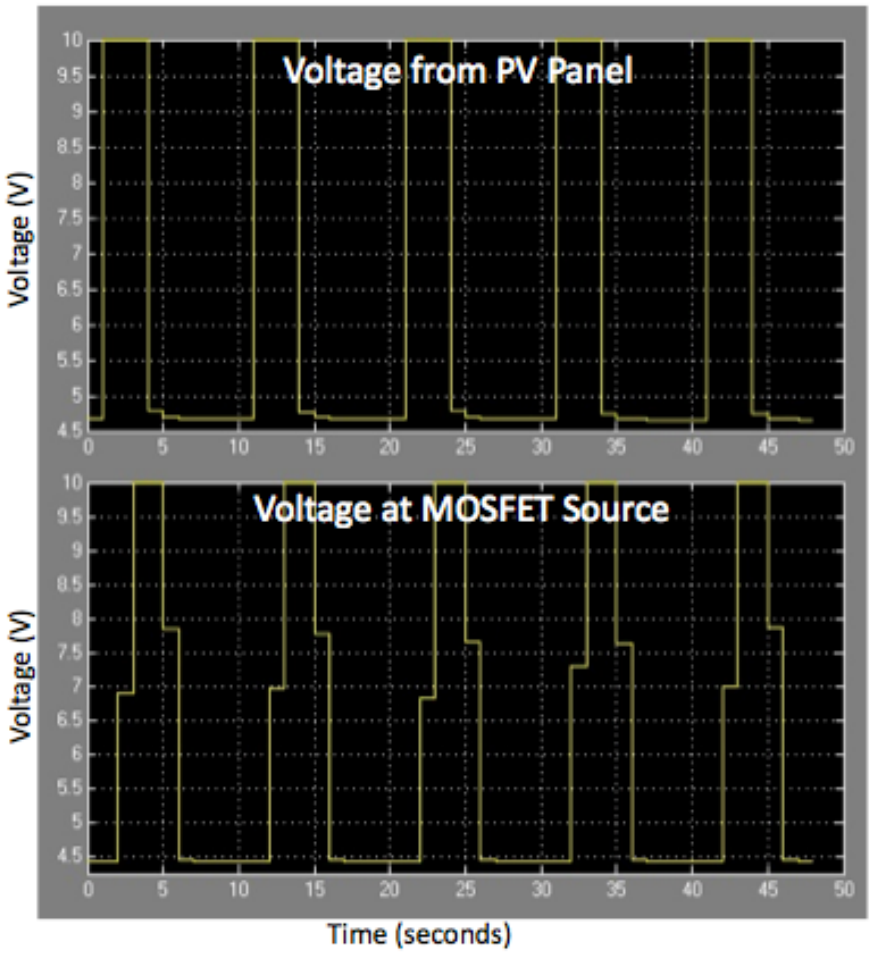

Figure 10: Sampling input voltages

9. Production Schedule

During the Fall term, research was done to better understand the need for MPPT devices and how they can be implemented. Initial testing was also done to characterize the solar panel for the project. Then calculations were done to determine starting values and component types.

Winter Term:

Week 1
- Collected parts and ordered battery

Week 2
- Began programming control system in Matlab, discovered the I/O card works best with Simulink

Week 3
- Refreshed knowledge of Simulink by watching tutorials
- Continued issues with the I/O card and Simulink communicating
- Constructed preliminary DC-to-DC circuit

Week 4
- Debugged circuit and added TTL gate and transistor level shifter stages
- Explored Simulink and talked to Professor Hodgson for assistance with the Real-Time Windows Target

Week 5
- Continued building control system in Simulink and testing it with constant inputs before connecting to the rest of the system

Week 6
- Continue refining Simulink block diagram and simulating different charging scenarios

Week 7
- Combined Simulink control with I/O card and circuitry with a power supply as input to the DC-to-DC converter

Week 8
- Combined all stages with the actual PV panel
- Prepared for presentation and demonstration session

Week 9
- Worked on final paper
- Debugged circuitry issues and ordered a schottky diode for the DC-to-DC converter

Week 10
- Continued work on paper
- Partially fixed issue with sampling time of analog inputs in Simulink

There were many problems getting an I/O card to work correctly with Simulink. If these issues had been sorted out sooner in the term, or during the fall, there would have been more time to test the project and make adjustments.

10. Cost Analysis

I was provided with all of the expensive parts of the project. The only components which were purchased specially for the project were the MOSFET, inductor and battery (bolded items in Table 1) totaling less than $25. The cost of all components and software comes to about $10,770. For a user without Simulink it would not make sense for them to purchase it for this application, the program could instead be put on a microcontroller from the Simulink control system to be manufactured.

MOSFET	**$2**
Inductor	**$10**
3.7V Lithium Ion Battery	**$10**
Other circuit components (diode, BJT, resistors, capacitor)	$15
Analog and Digital I/O Module NI PCI-6035E	$2,037
Computer	$600
Simulink with needed toolboxes	$3,400
Solar Panel	$75
Halogen Lamp	$20

Table 1: Components and Costs

11. User's Manual

The project is currently set up in the lab, with a light source which must initially be turned on for approximately one hour to allow the panel's surface temperature to stabilize. The user must attach the battery across the output of the circuit and the leads of the solar panel to the input of the circuit. Then they must turn the power supply on and press start on the Simulink program. The system will automatically stop the battery from charging when it is fully charged. This allows the user to leave the battery attached to the charger for as long as they desire. When the battery is then needed for use in an appliance the program can be stopped and the power supplies shut off. The battery can be taken out of the circuit to power a load and reattached to the charging circuit as needed.

This setup is for testing purposes and a manufactured version would use the natural sunlight to power a PV panel. The solar panel will need to be in direct sunlight to adequately charge the battery. Ideally the solar panel's leads would be permanently attached to the DC-to-DC converter. There would then be an easy way to attach the battery which the panel is going to charge. Lastly the Simulink program could be exported from Matlab to a portable microcontroller, using C+, and the external power supplies could be eliminated.

12. Discussion, Conclusions, and Recommendations

The constructed circuit and control algorithm have the ability to operate the solar panel at the largest possible power along a time-averaged line of current vs. voltage conditions. By most closely matching the impedance of the solar panel and battery the maximum power can be transferred from the solar panel to battery.

There is still work to be done to solve the sampling rate issue allowing for the control system to find the MPP of the time-averaged IV line. There are also ways to improve the efficiency of the Simulink block diagram. If the circuit is changed such that the resistance is variable, it will be able to serve as an impedance matching device to perturb the operating PV panel conditions along the IV curve. Once this is established, it will be able to locate the MPP of the IV curve which has a higher power output than the maximum value the system is currently looking for. To make the device more user friendly it should be exported from Matlab onto a microcontroller which would be able to run without the computer. This would allow for an owner to set up a small solar panel which they could attach a battery too when it needed charging.

There are many different types of solar panels and batteries, allowing for endless possible combinations of charging sources and loads. A more robust design could allow for multiple combinations to be used rather than a specific solar panel and battery combination. A buck-boost converter would need to be implemented so the circuit could decrease or increase the voltage from the panel to the battery depending on their sizes.

As mentioned in the alternative design section, there are numerous different algorithm options for locating the maximum power point that could be examined. Some

will reach the MPP more quickly and stick to the point rather than oscillate a step above and below this point. After implementing multiple algorithms it would be interesting to note the speed at which they are each able to maximize the power from the PV panel along with the complexity involved in each algorithm.

Time management was very important during the course of the project. The project had a series of stages starting with research and initial design, then construction and testing. Completing a project this large over the course of about 20 weeks was a new experience which allowed for a deeper understanding of the engineering design process. Having the option to choose a project in an area of interest, allowed for an increase of knowledge about renewable energy. Starting with little background in power electronics concepts, knowledge of DC-to-DC converters was gained. Overall, the project was an invaluable experience which will be helpful to look back on when completing future projects in the work force or graduate school.

13. Acknowledgments

I would like to thank my advisor, Professor Smith, for the initial guidance in the design, as well as the continued weekly and sometimes daily support while completing the project. Professor Hodgson played a large role in getting the I/O card to work with Simulink and helped set up the Real-Time Windows Target. I often consulted Gene Davison for help locating needed components for the construction of the circuit. I would also like to thank all my ECE professors and classmates for their input on various parts of the project.

14. References

[1] Appelbaum, J.; , "The Quality of Load Matching in a Direct-Coupling Photovoltaic System," *Power Engineering Review, IEEE* , vol.PER-7, no.12, pp.27-28, Dec. 1987.

[2] Electricity from: Solar Energy, http://www.powerscorecard.org, 2000.

[3] D. Anderson, Positive & Negative Effects of Solar Energy, http://greenliving.nationalgeographic.com.

[4] Boyang Hu; Sathiakumar, S.; , "Modeling of a new multiple input converter configuration for PV/battery system with MPPT," *Electronic and Mechanical Engineering and Information Technology (EMEIT), 2011 International Conference on* , vol.3, no., pp.1209-1214, 12-14 Aug. 2011.

[5] Kazmi, S.; Goto, H.; Ichinokura, O.; Hai-Jiao Guo; , "An improved and very efficient MPPT controller for PV systems subjected to rapidly varying atmospheric conditions and partial shading," *Power Engineering Conference, 2009. AUPEC 2009. Australasian Universities*, vol., no., pp.1-6, 27-30 Sept. 2009.

[6] Brito, M.; Galotto, L.; Sampaio, L.; Melo, G.; Canesin, C.; , "Evaluation of the Main MPPT Techniques for Photovoltaic Applications," *Industrial Electronics, IEEE Transactions on* , vol.PP, no.99, pp.1, 0.

[7] Faranda, R.; Leva S., "Energy comparison of MPPT techniques for PV Systems," WSEAS Transactions on Power Systems, Milano, Italy, Issue 6 Volume 3, June 2008.

[8] Qiang Mei; Mingwei Shan; Liying Liu; Guerrero, J.M.; , "A Novel Improved Variable Step-Size Incremental-Resistance MPPT Method for PV Systems,"*Industrial Electronics, IEEE Transactions on* , vol.58, no.6, pp.2427-2434, June 2011.

[9] Lithium-ion Battery Charging Basics, http://www.powerstream.com/li.htm.

[10] N. Mohan, T. M. Undeland, W. P. Robbins, "Power Electronics Converters, Applications, and Design," 3rd ed. John Wiley & Sons, Inc., 2003, ch 7, pp. 161-178.

15. Appendix

15.1 Plotting IV curves for the Solar Panel

Using potentiometers of values 10Ω, 50Ω, 200Ω and 1kΩ, in parallel with the panel, the current was measured through the potentiometer and the voltage across it. These values were plotted for three different lighting conditions shown in Figure 11. To keep the irradiance as constant as possible the lighting condition was first found that would give a short circuit current of about 300mA, and then the light fixture was tilted vertically, to decrease the light on the panel, decreasing the short circuit current to 200mA and then to 100mA.

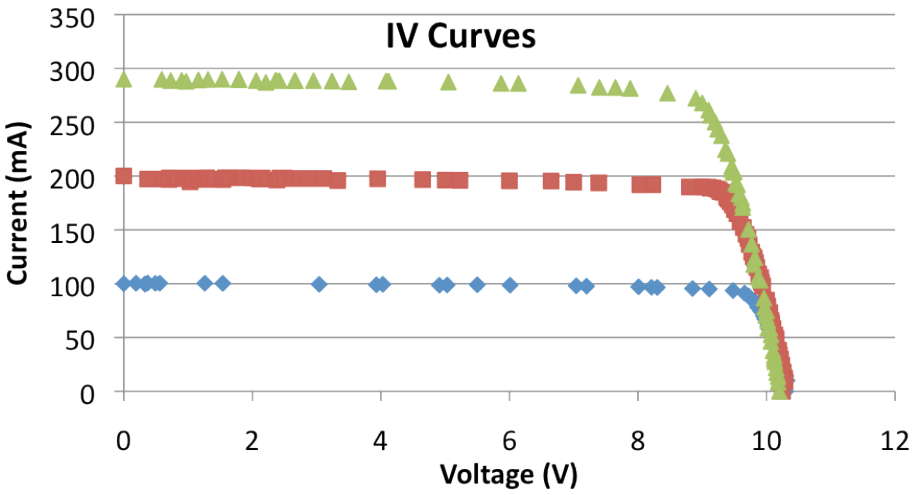

Figure 11: Plotted IV curves with halogen light source

Switching the MOSFET of the DC-to-DC converter the system can operate in an on or off state, corresponding to two points on the IV curve. The off state is at the open circuit voltage, since the I/O card is only able to read in up to 10V, this point will always be at 10V and no current. The on state is the point along the IV curve where the voltage is close to the battery's voltage. There are also voltage drops through the resistive components that must be taken into account. There are two 1.2Ω resistors and a

resistance of the MOSFET which was calculated to be 4.3Ω from the voltage drop from source to drain divided by a known current. Thus, the voltage of the on state will be (6.7Ω*current)+$V_{battery}$. Then varying the duty cycle takes the average value of the amount of time the panel's voltage operates at each of these points. The average value will be along a straight line between the two points. Figure 12 shows the IV curve and average value line with the line's maximum power point for one lighting condition and Figure 13 shows a different lighting intensity.

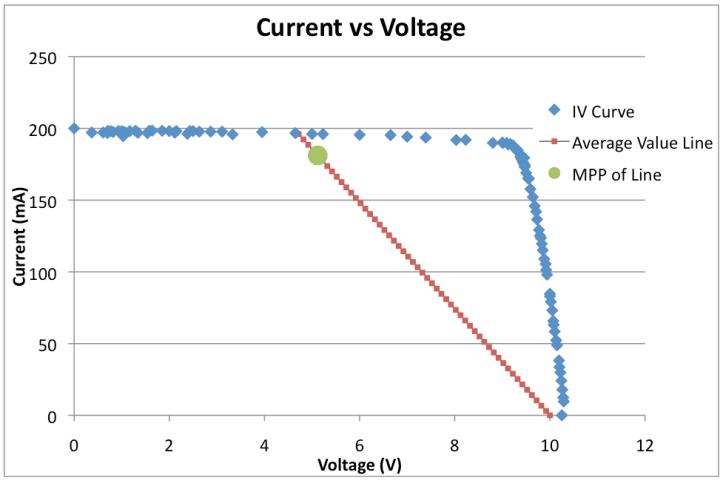

Figure 12: Time-average value line with MPP

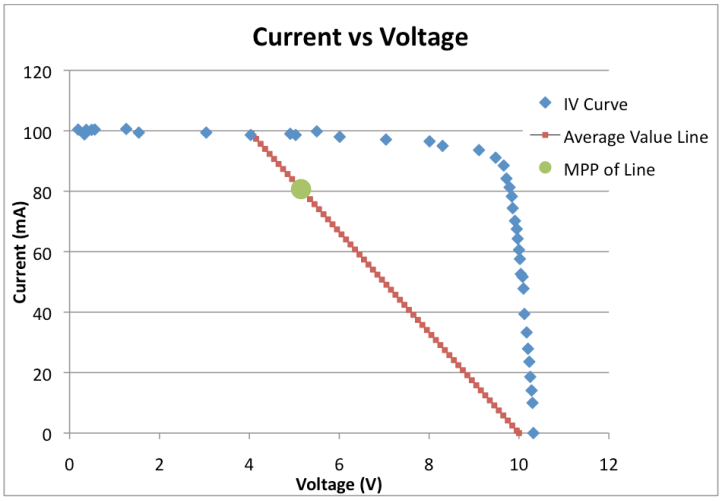

Figure 13: Time-average value line with MPP

15. 2 Simulink Block Diagram

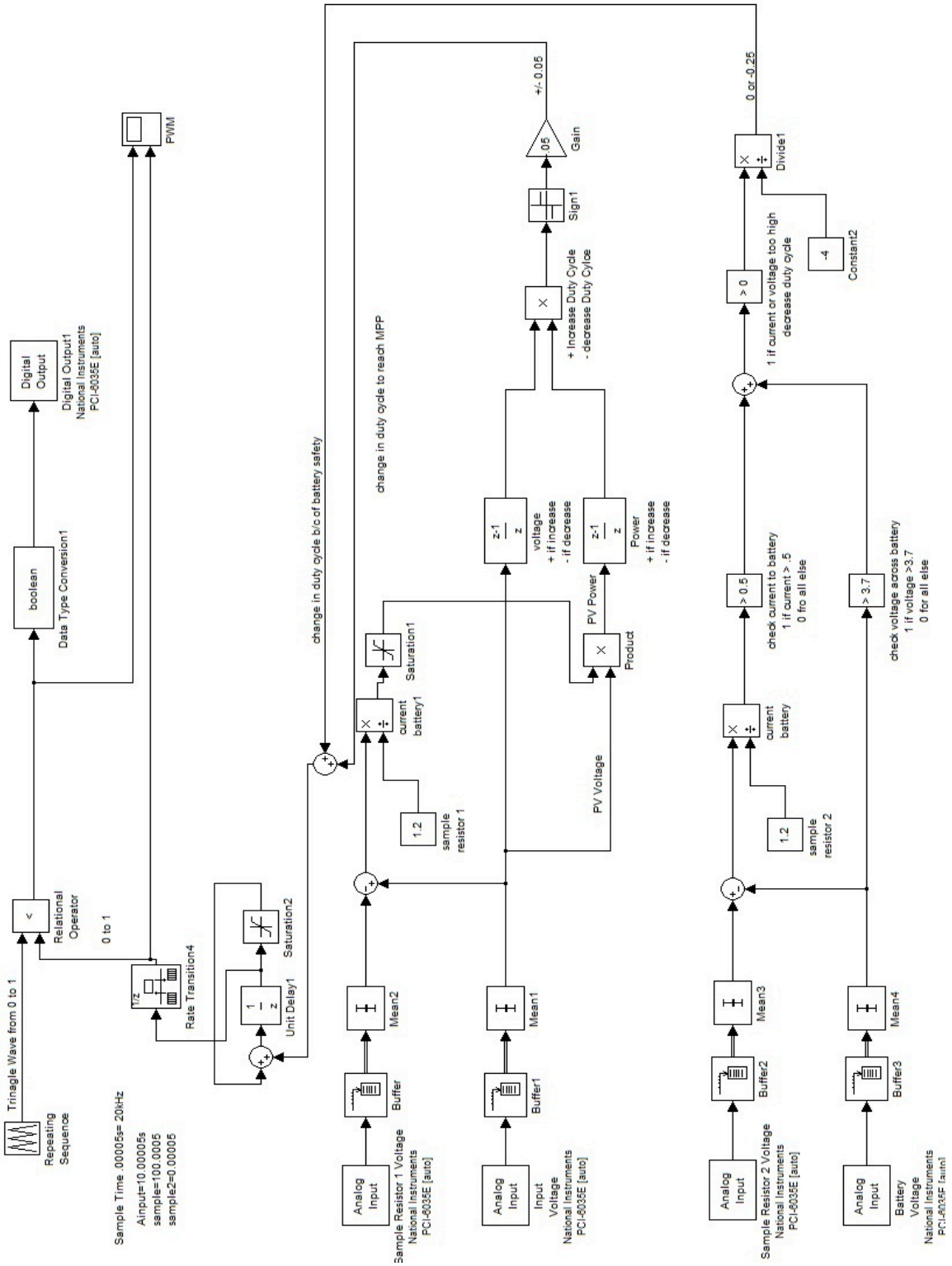

ELECTRONICS, INC.
44 FARRAND STREET
BLOOMFIELD, NJ 07003
(973) 748–5089

NTE2371
MOSFET
P–Ch, Enhancement Mode
High Speed Switch

Features:

- Dynamic dv/dt Rating
- Repetitive Avalanche Rated
- P–Channel
- Fast Switching
- Ease of Paralleling
- Simple Drive Requirements

Absolute Maximum Ratings:

Continuous Drain Current (V_{GS} = 10V), I_D
- T_C = +25°C 19A
- T_C = +100°C 13A

Pulsed Drain Current (Note 1), I_{DM} 72A

Power Dissipation (T_C = +25°C), P_D 150W
- Derate Linearly Above 25°C . . . . . 1.0W/°C

Gate–to–Source Voltage, V_{GS} . . . . . ±20

Single Pulse Avalanche Energy (Note 2), E_{AS} 640mJ

Avalanche Current (Note 1), I_{AR} 19A

Peak Diode Recovery dv/dt (Note 3), dv/dt 5.5V/ns

Operating Junction Temperature Range, T_J . . . . . –55° to +175°C

Storage Temperature Range, T_{stg} . . . . . –55° to +175°C

Lead Temperature (During Soldering, 1.6mm from case for 10sec), T_L . . . . . +300°C

Mounting Torque (6–32 or M3 Screw) . . . . . 10 lbf•in (1.1N•m)

Thermal Resistance, Junction–to–Case, R_{thJC} . . . . . 1.0°C/W

Thermal Resistance, Junction–to–Ambient, R_{thJA} . . . . . 62°C/W

Typical Thermal Resistance, Case–to–Sink (Flat, Greased Surface), R_{thCS} . . . . . 0.5°C/W

Note 1. Repetitive rating; pulse width limited by maximum junction temperature.

Note 2. V_{DD} = 25V, starting T_J = +25°C, L = 2.7mH, R_G = 25Ω, I_{AS} = 19A

Note 3. $I_{SD} \le$ 19A, di/dt ≤ 200A/μs, $V_{DD} \le V_{(BR)DSS}$, $T_J \le$ +175°C

Note 4. Pules Width ≤ 300μs, Duty Cycle ≤ 2%.

Electrical Characteristics: (T_J = +25°C unless otherwise specified)

Parameter	Symbol	Test Conditions	Min	Typ	Max	Unit
Drain–to–Source Breakdown Voltage	$V_{(BR)DSS}$	V_{GS} = 0V, I_D = 250μA	100	–	–	V
Breakdown Voltage Temp. Coefficient	$\frac{\Delta V_{(BR)DSS}}{\Delta T_J}$	Reference to +25°C, I_D = 1mA	–	0.087	–	V/°C
Static Drain–to–Source On–Resistance	$R_{DS(on)}$	V_{GS} = 10V, I_D = 11A, Note 4	–	–	0.20	Ω
Gate Threshold Voltage	$V_{GS(th)}$	V_{DS} = V_{GS}, I_D = 250μA	2.0	–	4.0	V
Forward Transconductance	g_{fs}	V_{DS} = 50V, I_D = 11A, Note4	6.2	–	–	mhos
Drain–to–Source Leakage Current	I_{DSS}	V_{DS} = 100V, V_{GS} = 0V	–	–	100	μA
		V_{DS} = 80V, V_{GS} = 0V, T_J = +150°C	–	–	500	μA
Gate–to–Source Forward Leakage	I_{GSS}	V_{GS} = –20V	–	–	–100	nA
Gate–to–Source Reverse Leakage	I_{GSS}	V_{GS} = 20V	–	–	100	nA
Total Gate Charge	Q_g	I_D = 19A, V_{DS} = 80V, V_{GS} = 10V, Note 4	–	–	61	nC
Gate–to–Source Charge	Q_{gs}		–	–	14	nC
Gate–to–Drain (“Miller”) Charge	Q_{gd}		–	–	29	nC
Turn–On Delay Time	$t_{d(on)}$	V_{DD} = 50V, I_D = 19A, R_G = 9.1Ω, R_D = 2.4Ω, Note 4	–	16	–	ns
Rise Time	t_r		–	73	–	ns
Turn–Off Delay Time	$t_{d(off)}$		–	34	–	ns
Fall Time	t_f		–	57	–	ns
Internal Drain Inductance	L_D	Between lead, .250in. (6.0) mm from package and center of die contact	–	4.5	–	nH
Internal Source Inductance	L_S		–	7.5	–	nH
Input Capacitance	C_{iss}	V_{GS} = 0V, V_{DS} = 25V, f = 1MHz	–	1400	–	pF
Output Capacitance	C_{oss}		–	590	–	pF
Reverse Transfer Capaticance	C_{rss}		–	140	–	pF

Source–Drain Ratings and Characteristics:

Parameter	Symbol	Test Conditions	Min	Typ	Max	Unit
Continuous Source Current (Body Diode)	I_S		–	–	19	A
Pulsed Source Current (Body Diode)	I_{SM}	Note 1	–	–	72	A
Diode Forward Voltage	V_{SD}	T_J = +25°C, I_S = 3.5A, V_{GS} = 0V, Note 3	–	–	5.0	V
Reverse Recovery Time	t_{rr}	T_J = +25°C, I_F = 3.5A, di/dt = 100A/μs, Note 3	–	130	260	ns
Reverse Recovery Charge	Q_{rr}		–	0.35	0.70	μC
Forward Turn–On Time	t_{on}	Intrinsic turn–on time is neglegible (turn–on is dominated by L_S+L_D)				

Note 1. Repetitive rating; pulse width limited by maximum junction temperature.

Note 4. Pulse width ≤ 300μs; duty cycle ≤ 2%.

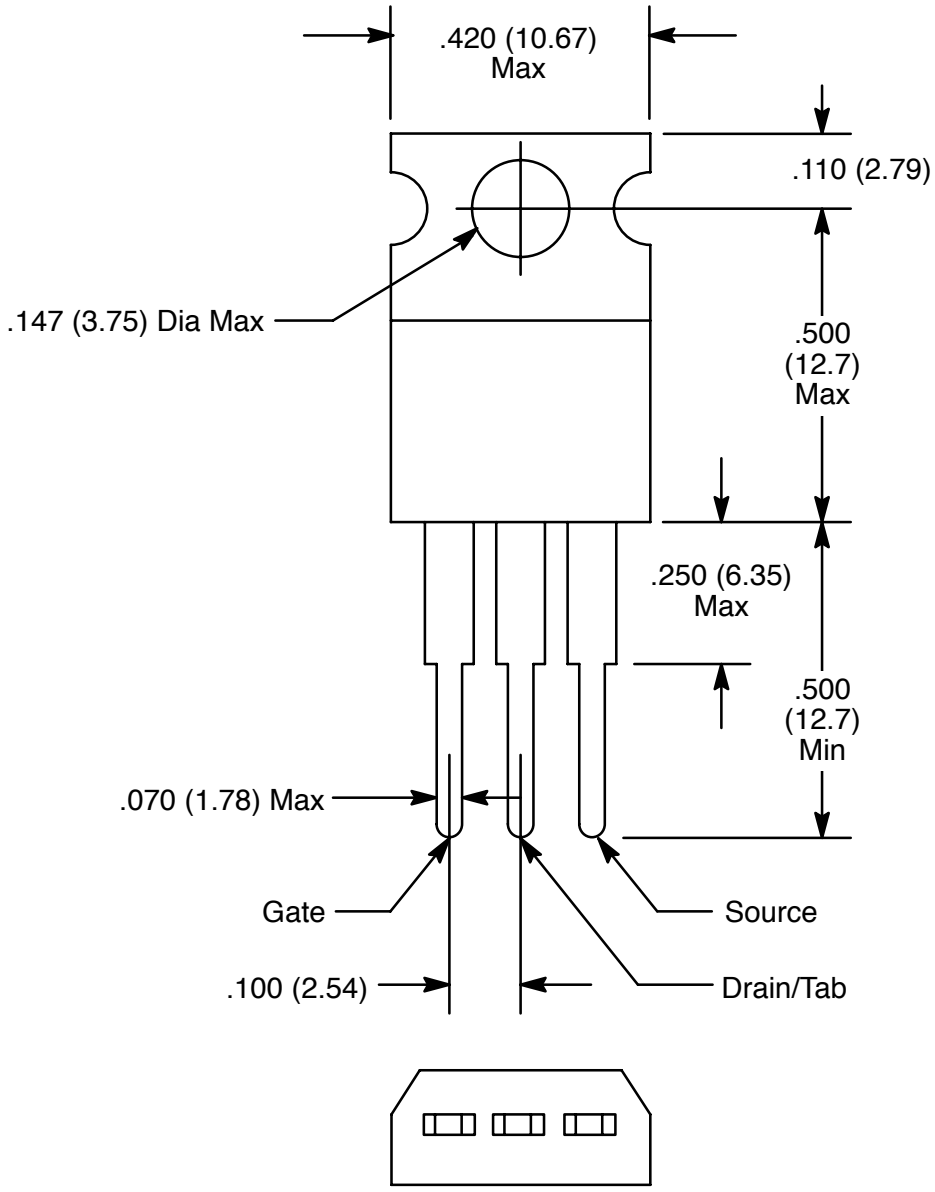
.420 (10.67)
Max
.110 (2.79)
.147 (3.75) Dia Max
.500
(12.7)
Max
.250 (6.35)
Max
.500
(12.7)
Min
.070 (1.78) Max
Gate
Source
.100 (2.54)
Drain/Tab

MOTOROLA
SEMICONDUCTOR TECHNICAL DATA

Order this document
by 1N5817/D

Axial Lead Rectifiers

. . . employing the Schottky Barrier principle in a large area metal–to–silicon power diode. State–of–the–art geometry features chrome barrier metal, epitaxial construction with oxide passivation and metal overlap contact. Ideally suited for use as rectifiers in low–voltage, high–frequency inverters, free wheeling diodes, and polarity protection diodes.

- Extremely Low v_F
- Low Stored Charge, Majority Carrier Conduction
- Low Power Loss/High Efficiency

Mechanical Characteristics

- Case: Epoxy, Molded
- Weight: 0.4 gram (approximately)
- Finish: All External Surfaces Corrosion Resistant and Terminal Leads are Readily Solderable
- Lead and Mounting Surface Temperature for Soldering Purposes: 220°C Max. for 10 Seconds, 1/16″ from case
- Shipped in plastic bags, 1000 per bag.
- Available Tape and Reeled, 5000 per reel, by adding a “RL” suffix to the part number
- Polarity: Cathode Indicated by Polarity Band
- Marking: 1N5817, 1N5818, 1N5819

1N5817
1N5818
1N5819

1N5817 and 1N5819 are Motorola Preferred Devices

SCHOTTKY BARRIER RECTIFIERS
1 AMPERE
20, 30 and 40 VOLTS

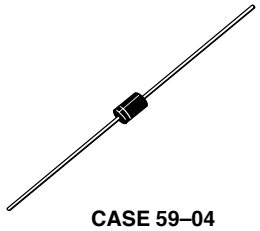

CASE 59–04

MAXIMUM RATINGS

Rating	Symbol	1N5817	1N5818	1N5819	Unit
Peak Repetitive Reverse Voltage Working Peak Reverse Voltage DC Blocking Voltage	V_{RRM} V_{RWM} V_R	20	30	40	V
Non–Repetitive Peak Reverse Voltage	V_{RSM}	24	36	48	V
RMS Reverse Voltage	$V_{R(RMS)}$	14	21	28	V
Average Rectified Forward Current (2) ($V_{R(equiv)} \le 0.2\ V_R(dc)$, T_L = 90°C, $R_{\theta JA}$ = 80°C/W, P.C. Board Mounting, see Note 2, T_A = 55°C)	I_O	1.0			A
Ambient Temperature (Rated $V_R(dc)$, $P_{F(AV)} = 0$, $R_{\theta JA}$ = 80°C/W)	T_A	85	80	75	°C
Non–Repetitive Peak Surge Current (Surge applied at rated load conditions, half–wave, single phase 60 Hz, T_L = 70°C)	I_{FSM}	25 (for one cycle)			A
Operating and Storage Junction Temperature Range (Reverse Voltage applied)	T_J, T_{stg}	–65 to +125			°C
Peak Operating Junction Temperature (Forward Current applied)	$T_{J(pk)}$	150			°C

THERMAL CHARACTERISTICS (2)

Characteristic	Symbol	Max	Unit
Thermal Resistance, Junction to Ambient	$R_{\theta JA}$	80	°C/W

ELECTRICAL CHARACTERISTICS (T_L = 25°C unless otherwise noted) (2)

Characteristic		Symbol	1N5817	1N5818	1N5819	Unit
Maximum Instantaneous Forward Voltage (1)	(i_F = 0.1 A) (i_F = 1.0 A) (i_F = 3.0 A)	v_F	0.32 0.45 0.75	0.33 0.55 0.875	0.34 0.6 0.9	V
Maximum Instantaneous Reverse Current @ Rated dc Voltage (1)	(T_L = 25°C) (T_L = 100°C)	I_R	1.0 10	1.0 10	1.0 10	mA

(1) Pulse Test: Pulse Width = 300 μs, Duty Cycle = 2.0%.
(2) Lead Temperature reference is cathode lead 1/32″ from case.

Preferred devices are Motorola recommended choices for future use and best overall value.

NOTE 1 — DETERMINING MAXIMUM RATINGS

Reverse power dissipation and the possibility of thermal runaway must be considered when operating this rectifier at reverse voltages above 0.1 V_{RWM}. Proper derating may be accomplished by use of equation (1).

$$T_{A(max)} = T_{J(max)} - R_{\theta JA}P_{F(AV)} - R_{\theta JA}P_{R(AV)} \quad (1)$$

where $T_{A(max)}$ = Maximum allowable ambient temperature
$T_{J(max)}$ = Maximum allowable junction temperature (125°C or the temperature at which thermal runaway occurs, whichever is lowest)
$P_{F(AV)}$ = Average forward power dissipation
$P_{R(AV)}$ = Average reverse power dissipation
$R_{\theta JA}$ = Junction–to–ambient thermal resistance

Figures 1, 2, and 3 permit easier use of equation (1) by taking reverse power dissipation and thermal runaway into consideration. The figures solve for a reference temperature as determined by equation (2).

$$T_R = T_{J(max)} - R_{\theta JA}P_{R(AV)} \quad (2)$$

Substituting equation (2) into equation (1) yields:

$$T_{A(max)} = T_R - R_{\theta JA}P_{F(AV)} \quad (3)$$

Inspection of equations (2) and (3) reveals that T_R is the ambient temperature at which thermal runaway occurs or where T_J = 125°C, when forward power is zero. The transition from one boundary condition to the other is evident on the curves of Figures 1, 2, and 3 as a difference in the rate of change of the slope in the vicinity of 115°C. The data of Figures 1, 2, and 3 is based upon dc conditions. For use in common rectifier circuits, Table 1 indicates suggested factors for an equivalent dc voltage to use for conservative design, that is:

$$V_{R(equiv)} = V_{in(PK)} \times F \quad (4)$$

The factor F is derived by considering the properties of the various rectifier circuits and the reverse characteristics of Schottky diodes.

EXAMPLE: Find $T_{A(max)}$ for 1N5818 operated in a 12–volt dc supply using a bridge circuit with capacitive filter such that I_{DC} = 0.4 A ($I_{F(AV)}$ = 0.5 A), $I_{(FM)}/I_{(AV)}$ = 10, Input Voltage = 10 $V_{(rms)}$, $R_{\theta JA}$ = 80°C/W.

Step 1. Find $V_{R(equiv)}$. Read F = 0.65 from Table 1,
$\therefore V_{R(equiv)} = (1.41)(10)(0.65) = 9.2$ V.
Step 2. Find T_R from Figure 2. Read T_R = 109°C
@ V_R = 9.2 V and $R_{\theta JA}$ = 80°C/W.
Step 3. Find $P_{F(AV)}$ from Figure 4. **Read $P_{F(AV)}$ = 0.5 W

$$@ \frac{I_{(FM)}}{I_{(AV)}} = 10 \text{ and } I_{F(AV)} = 0.5 \text{ A.}$$

Step 4. Find $T_{A(max)}$ from equation (3).
$T_{A(max)} = 109 - (80)(0.5) = 69$°C.

**Values given are for the 1N5818. Power is slightly lower for the 1N5817 because of its lower forward voltage, and higher for the 1N5819.

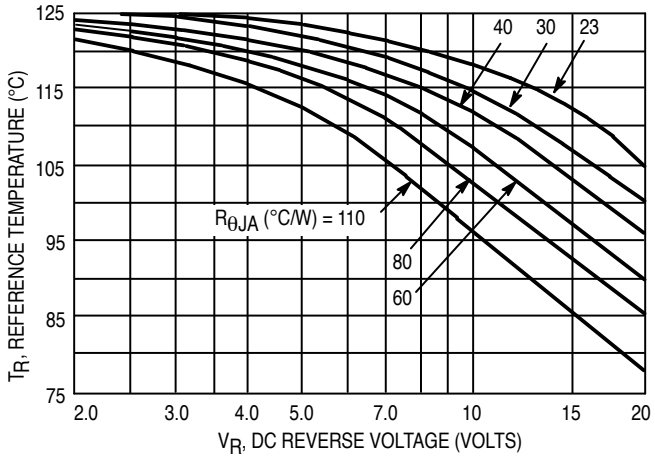

Figure 1. Maximum Reference Temperature 1N5817

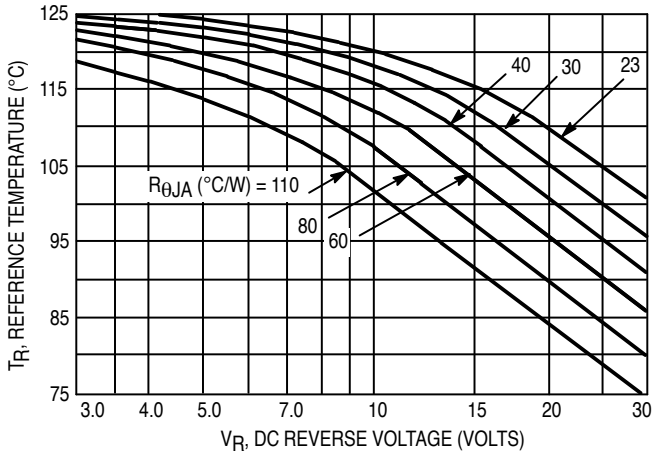

Figure 2. Maximum Reference Temperature 1N5818

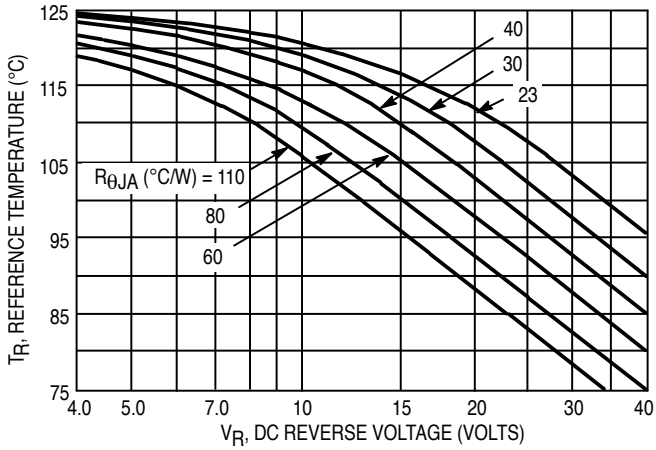

Figure 3. Maximum Reference Temperature 1N5819

Table 1. Values for Factor F

Circuit	Half Wave		Full Wave, Bridge		Full Wave, Center Tapped*†	
Load	Resistive	Capacitive*	Resistive	Capacitive	Resistive	Capacitive
Sine Wave	0.5	1.3	0.5	0.65	1.0	1.3
Square Wave	0.75	1.5	0.75	0.75	1.5	1.5

*Note that $V_{R(PK)} \approx 2.0\ V_{in(PK)}$. † Use line to center tap voltage for V_{in}.

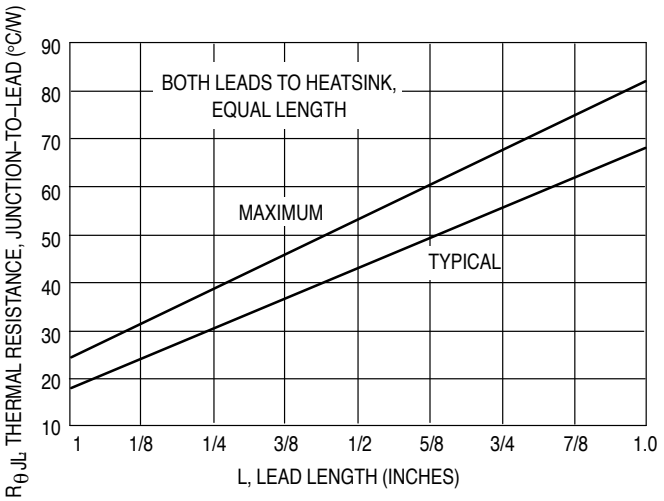

Figure 4. Steady–State Thermal Resistance

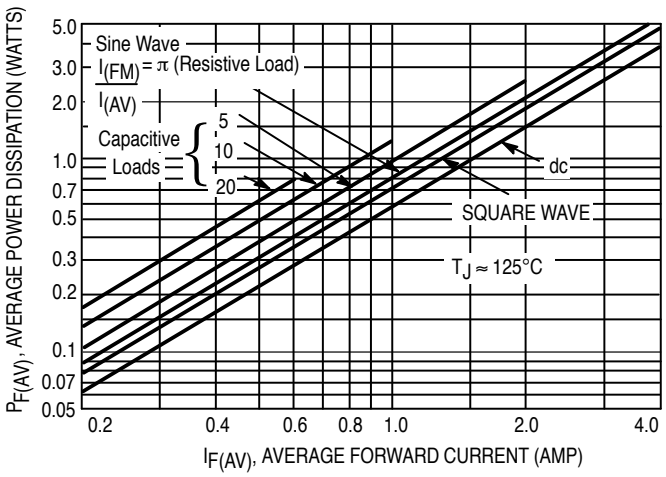

Figure 5. Forward Power Dissipation 1N5817–19

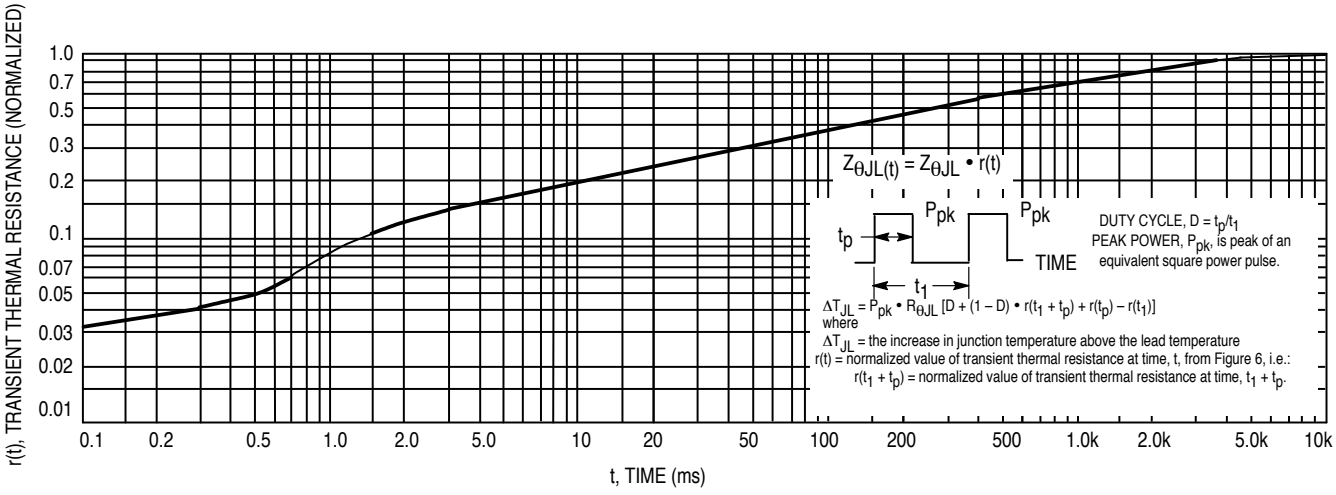

Figure 6. Thermal Response

NOTE 2 — MOUNTING DATA

Data shown for thermal resistance junction–to–ambient ($R_{\theta JA}$) for the mountings shown is to be used as typical guideline values for preliminary engineering, or in case the tie point temperature cannot be measured.

TYPICAL VALUES FOR $R_{\theta JA}$ IN STILL AIR

Mounting Method	Lead Length, L (in)				$R_{\theta JA}$
	1/8	1/4	1/2	3/4	
1	52	65	72	85	°C/W
2	67	80	87	100	°C/W
3	50				°C/W

Mounting Method 1

P.C. Board with 1–1/2″ x 1–1/2″ copper surface.

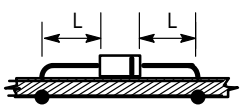

Mounting Method 3

P.C. Board with 1–1/2″ x 1–1/2″ copper surface.

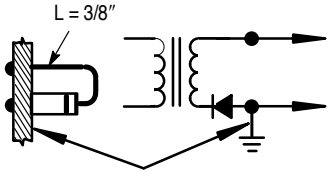

Mounting Method 2

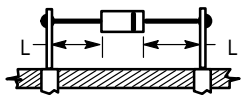

VECTOR PIN MOUNTING

NOTE 3 — THERMAL CIRCUIT MODEL
(For heat conduction through the leads)

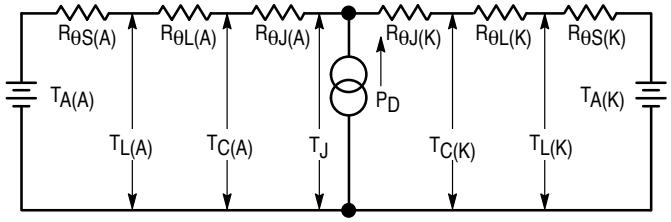

Use of the above model permits junction to lead thermal resistance for any mounting configuration to be found. For a given total lead length, lowest values occur when one side of the rectifier is brought as close as possible to the heatsink. Terms in the model signify:

T_A = Ambient Temperature T_C = Case Temperature
T_L = Lead Temperature T_J = Junction Temperature
$R_{\theta S}$ = Thermal Resistance, Heatsink to Ambient
$R_{\theta L}$ = Thermal Resistance, Lead to Heatsink
$R_{\theta J}$ = Thermal Resistance, Junction to Case
P_D = Power Dissipation

(Subscripts A and K refer to anode and cathode sides, respectively.)
Values for thermal resistance components are:
$R_{\theta L}$ = 100°C/W/in typically and 120°C/W/in maximum
$R_{\theta J}$ = 36°C/W typically and 46°C/W maximum.

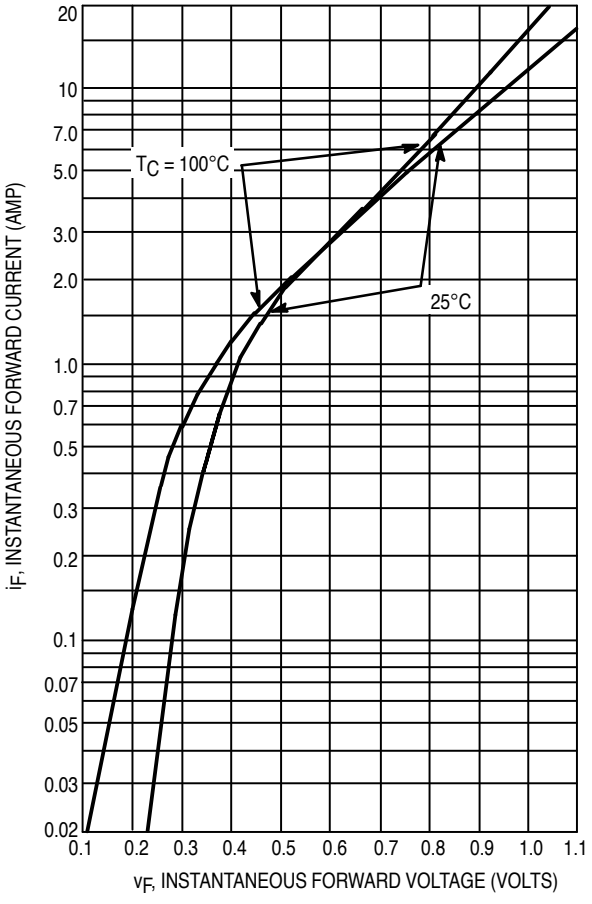

Figure 7. Typical Forward Voltage

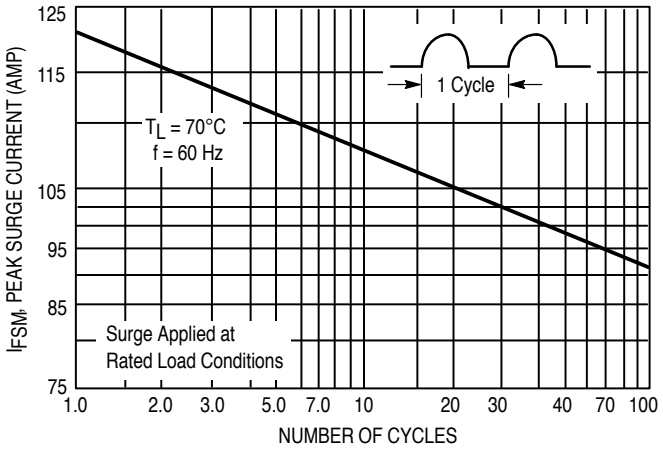

Figure 8. Maximum Non–Repetitive Surge Current

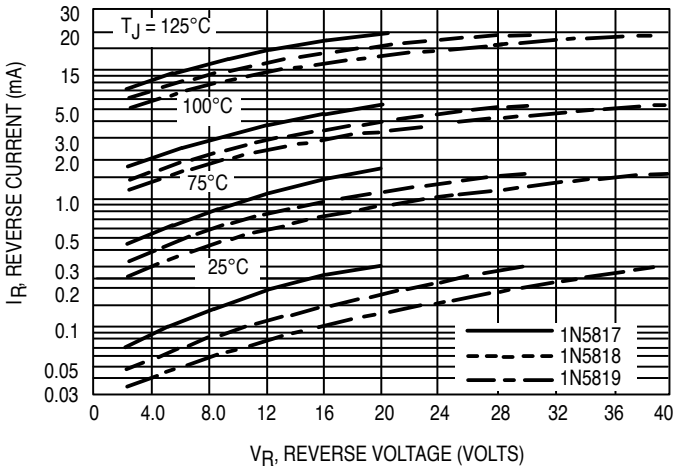

Figure 9. Typical Reverse Current

NOTE 4 — HIGH FREQUENCY OPERATION

Since current flow in a Schottky rectifier is the result of majority carrier conduction, it is not subject to junction diode forward and reverse recovery transients due to minority carrier injection and stored charge. Satisfactory circuit analysis work may be performed by using a model consisting of an ideal diode in parallel with a variable capacitance. (See Figure 10.)

Rectification efficiency measurements show that operation will be satisfactory up to several megahertz. For example, relative waveform rectification efficiency is approximately 70 percent at 2.0 MHz, e.g., the ratio of dc power to RMS power in the load is 0.28 at this frequency, whereas perfect rectification would yield 0.406 for sine wave inputs. However, in contrast to ordinary junction diodes, the loss in waveform efficiency is not indicative of power loss: it is simply a result of reverse current flow through the diode capacitance, which lowers the dc output voltage.

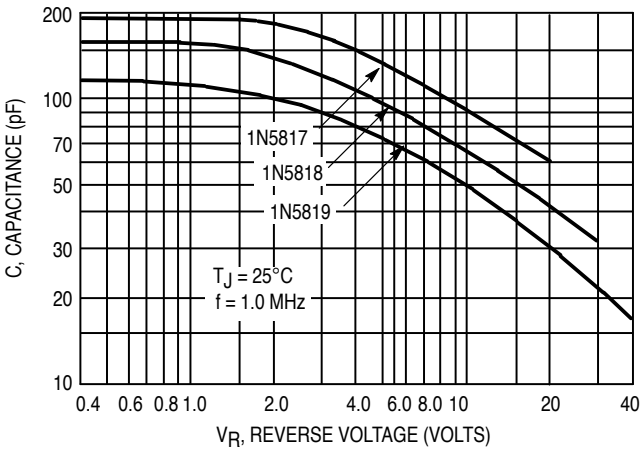

Figure 10. Typical Capacitance

PACKAGE DIMENSIONS

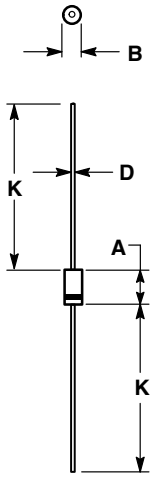

NOTES:
1. ALL RULES AND NOTES ASSOCIATED WITH JEDEC DO–41 OUTLINE SHALL APPLY.
2. POLARITY DENOTED BY CATHODE BAND.
3. LEAD DIAMETER NOT CONTROLLED WITHIN F DIMENSION.

	MILLIMETERS		INCHES	
DIM	MIN	MAX	MIN	MAX
A	5.97	6.60	0.235	0.260
B	2.79	3.05	0.110	0.120
D	0.76	0.86	0.030	0.034
K	27.94	—	1.100	—

CASE 59–04
ISSUE M

How to reach us:
USA/EUROPE/Locations Not Listed: Motorola Literature Distribution; P.O. Box 5405, Denver, Colorado 80217. 303–675–2140 or 1–800–441–2447

Mfax™: RMFAX0@email.sps.mot.com – TOUCHTONE 602–244–6609
INTERNET: http://Design–NET.com

JAPAN: Nippon Motorola Ltd.; Tatsumi–SPD–JLDC, 6F Seibu–Butsuryu–Center, 3–14–2 Tatsumi Koto–Ku, Tokyo 135, Japan. 81–3–3521–8315

ASIA/PACIFIC: Motorola Semiconductors H.K. Ltd.; 8B Tai Ping Industrial Park, 51 Ting Kok Road, Tai Po, N.T., Hong Kong. 852–26629298